Formation of C-S-H in calcium hydroxide–blast furnace slag– quartz–water system in autoclaving conditions

Nourredine Arabi, Nourredine Chelghoum, Raoul Jauberthie, Laurent Molez

▶ **To cite this version:**

Nourredine Arabi, Nourredine Chelghoum, Raoul Jauberthie, Laurent Molez. Formation of C-S-H in calcium hydroxide–blast furnace slag– quartz–water system in autoclaving conditions. Advances in Cement Research, 2015, 27 (3), pp.153-162. 10.1680/adcr.13.00069 . hal-01366494

HAL Id: hal-01366494
https://hal.science/hal-01366494

Submitted on 14 Sep 2016

HAL is a multi-disciplinary open access archive for the deposit and dissemination of scientific research documents, whether they are published or not. The documents may come from teaching and research institutions in France or abroad, or from public or private research centers.

L'archive ouverte pluridisciplinaire **HAL**, est destinée au dépôt et à la diffusion de documents scientifiques de niveau recherche, publiés ou non, émanant des établissements d'enseignement et de recherche français ou étrangers, des laboratoires publics ou privés.

Advances in Cement Research
Volume 27 Issue 3

Formation of C-S-H in calcium hydroxide–blast furnace slag–quartz–water system in autoclaving conditions
Arabi, Jauberthie, Chelghoum and Molez

Advances in Cement Research, 2015, **27**(3), 153–162
http://dx.doi.org/10.1680/adcr.13.00069
Paper 1300069
Received 30/09/2013; revised 03/12/2013; accepted 06/12/2013
Published online ahead of print 15/02/2014

ICE Publishing: All rights reserved

ice
Institution of Civil Engineers
publishing

Formation of C-S-H in calcium hydroxide–blast furnace slag–quartz–water system in autoclaving conditions

Nourredine Arabi
Professor, Laboratoire Matériaux Géomatériaux et Environnement, Université Badji Mokhtar Annaba, Annaba, Algeria

Raoul Jauberthie
Professor, Laboratoire GCGM, INSA de Rennes, Rennes, France

Nourredine Chelghoum
Senior lecturer, Laboratoire Matériaux Géomatériaux et Environnement, Université Badji Mokhtar Annaba, Annaba, Algeria

Laurent Molez
Senior lecturer, Laboratoire GCGM, INSA de Rennes, Rennes, France

In masonry, the most commonly used materials are concrete blocks or burnt clay brick. Owing to energy costs, there is a need to explore alternative raw materials and energy-efficient technologies for making building materials. This paper deals with the incorporation of blast furnace granulated slag in sand–lime materials as a replacement for hydrated lime during autoclaving conditions. The slag grain-size grinding and the heat treatment in saturated vapour pressure autoclave conditions were investigated to study the compressive strength behaviour of the new material. This substitution induces a decrease in compressive strength. The reaction products consist mainly of 11 nm tobermorite and xonotlite. The X-ray diffractions of these phases are difficult to see. The slag seems more reactive with lime than quartz. Observations with the scanning electron microscope allow better appreciation of these crystallites. With its composition and amorphous structure, the granulated slag does not release new distinct phases of hydrates.

Introduction

Calcium silicate hydrate (C-S-H) is formed during paste hydration of the tricalcium silicate (C_3S) and dicalcium silicate (C_2S) phase in Portland cement paste at ordinary temperatures. The formed C-S-H is of amorphous or poorly crystalline form and has a wide compositional range, with molar calcium oxide (CaO)/silicon dioxide (SiO_2) (C/S) ratios between 0·6 and more than 2 (Aitken and Taylor, 1960; Al-Wakeel *et al.*, 1999; Chen *et al.*, 2004).

The lime silica water has been investigated in autoclaving conditions at different temperatures and during reactions by different authors. The stability is sometimes questioned after several years. This system is highly complex with over 30 stable phases reported. The relative stabilities of some of these phases are shown in Figure 1 (Taylor, 1997). The C/S ratios of C-S-H precipitated from aqueous solution depend on the C/S ratios of the starting materials, with higher C/S ratios in the starting materials usually resulting in higher C/S ratios in the final products (Baltakys *et al.*, 2009).

High-pressure steam curing adds remarkable features in comparison to cement hydration at lower temperatures. During autoclaving, some crystallised calcium silicate hydrates are formed. The crystal structure provides various building materials with highly

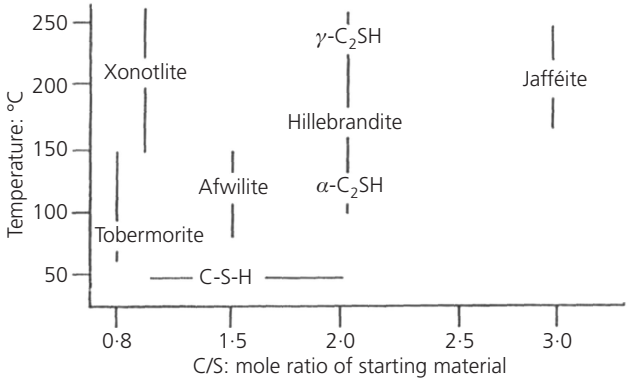

Figure 1. Taylor diagram: C-S-H depending on calcium oxide/silicon dioxide ratio at various temperatures

preferred properties, such as high strength, dimensional stability (shrink and creep) and high resistance to chemical attack (Richardson, 2008). In the majority of cases the product of transformation presents a mixture of C-S-H (I) and tobermorite (Hong and Glasser, 2004). Meanwhile, C-S-H (I) with crystals only ordered in two directions transforms to other phases (Z-phase) and then finally recrystallises to gyrolite (Jauberthie *et al.*, 1996; Klimesch and Ray, 2002; Siauciunas and Baltakys, 2004).

Offprint provided courtesy of www.icevirtuallibrary.com
Author copy for personal use, not for distribution

C-S-H (I) can be an intermediate phase in the formation of the other phases mentioned. For other C/S ratios or other atoms present, with higher temperature (150°C) tobermorite transforms to xonotlite (Shaw *et al.*, 2000).

Sand–lime brick is obtained by hydrothermal reaction of a mixture of lime and sand at high temperatures under saturation vapour pressure in an autoclave (Kondo, 1965). At temperatures around 170–200°C, the finely ground quartz which is insoluble at room temperature becomes chemically more active and reacts with lime 'calcium hydroxide ($Ca(OH)_2$)', thereby forming C-S-H that is solid, resistant and insoluble in water. However, despite many previous studies, several aspects of the reaction are still incompletely understood. This reaction type is often affected according to the duration or too high temperature of autoclaving or by the presence of too much fine quartz (Crennan *et al.*, 1977).

The hydrothermal process in the autoclave is still not fully scientifically understood. The difficulties in following the process in the autoclave are mainly attributable to the 'black box'; that is, the synthesis in an autoclave cannot be observed (Dietz and Bohnemann, 2000). However, the C-S-H formed at ambient temperatures is amorphous or poorly crystallised, whereas the autoclaved calcium silicate hydrate is mostly well crystallised. The degree of crystallisation depends on the raw materials, C/S ratio, curing conditions in the autoclave and other factors (Yazıcı *et al.*, 2013). Temperature and time of autoclaving determine which form of C-S-H is produced. The relevant forms of C-S-H in autoclaved building materials are 11 nm tobermorite and xonotlite. The 11 nm tobermorite is more stable, is obtained at 0·8–1 C/S ratio and is synthesised at temperatures above 150°C, whereas the xonotlite, formed by the molar C/S ratio of approximately 1, is produced at temperatures above 200°C (Black *et al.*, 2009).

The C-S-H synthesis starts with the dissolution of the raw materials (calcium hydroxide and silicon dioxide). The calcium hydroxide dissolves in the aqueous phase (Ca^{2+} and OH^-) and the silicon dioxide dissolves in the aqueous phase as $(H_3SiO_4)^-$ or $(H_2SiO_4)^{2-}$ complexes. The solubility kinetics of calcium hydroxide and silicon dioxide are shown in Figure 2 (Dietz and Bohnemann, 2000). At lower temperatures the solubility of the calcium hydroxide in comparison to the silicon dioxide is far higher. This is the reason why the initially produced C-S-H is lime-rich or semi-crystalline C-S-H with a C/S ratio of more than 1·5. At higher temperatures the silicon dioxide solubility is increased, whereas the solubility of the calcium oxide is decreased. All the dissolved silicon dioxide is immediately consumed and it is the formation of 11 nm tobermorite which is favoured. Consequently the rate of reaction depends on the availability of dissolved silicon dioxide only (Narayanan and Ramamurthy, 2000; Ungkoon *et al.*, 2007). Significant influences have impurities in the raw materials, which can accelerate or inhibit the formation of the crystallised C-S-H. The

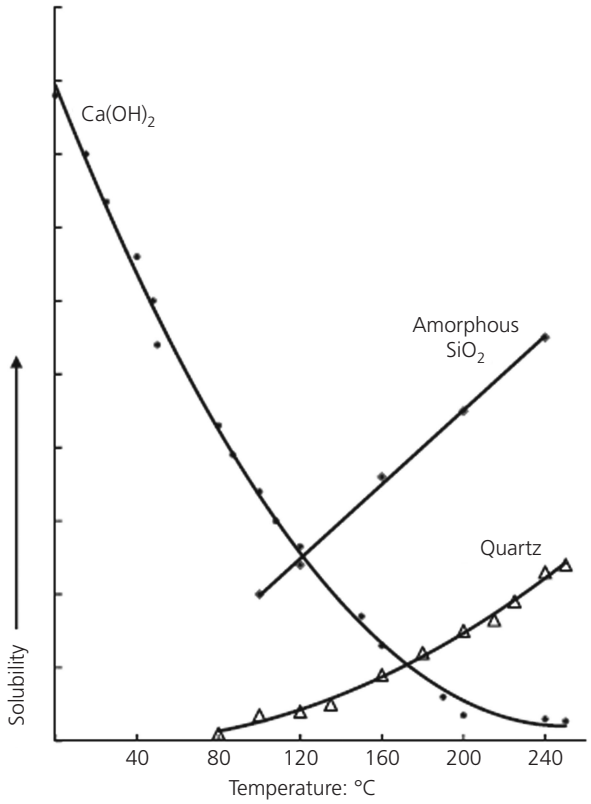

Figure 2. Solubility of calcium hydroxide and silicon dioxide in water at different temperatures

presence of some sulfates and aluminates enhance the formation of tobermorite, whereas the formation of xonotlite is inhibited by the presence of aluminium oxide (Dietz and Bohnemann, 2000).

With its chemical composition similar to cement, ground granulated blast furnace slag may be an alternative to lime materials. The rapid cooling gives a metastable glassy structure, which increases the kinetic of the reaction with the lime. Granulated slag has latent hydraulic properties, it is considered to be slow curing and it is not reactive with water at room temperature (Behim *et al.*, 2011). Chemical activation, sulfate or alkali are necessary to start germination (Gruskovnjak *et al.*, 2008). Furthermore, the slag can also become reactive with thermal activation (steaming or autoclaving) (Barnett *et al.*, 2006).

In this work, the lime and granulated slag were mixed with different composition, and the reaction occurred at the saturated vapour pressure at various temperatures. Slag grinding degree characterised by the Blaine specific surface was investigated. Mechanical performance was evaluated by compressive strength. Analysis by X-ray diffraction (XRD), X-ray microanalysis (EDX) and scanning electron microscope (SEM) observations explained the evolution of phases obtained during autoclave reaction.

Offprint provided courtesy of www.icevirtuallibrary.com
Author copy for personal use, not for distribution

Experimental details

Materials

The materials used in this work are outlined below.

(*a*) Calcium hydroxide (industrial product of ArcelorMittal in El Hadjar, Algeria). This was used with a particle size distribution giving a screen overflow of 19·2% on the 0·08 mm sieve.
(*b*) Blast furnace slag is a by-product of the iron industry ArcelorMittal in El Hadjar (Algeria). It was ground to obtain different Blaine specific surfaces (SSB) to 2500, 3500 and 4500 cm^2/g.
(*c*) Dune sand is quartz sand (El Kala, eastern Algeria). The particle size is reduced by ball milling to obtain a specific surface of 2325 cm^2/g.

All chemical analyses are summarised in Table 1 and are determined by manufacturer laboratory tests by the X-ray fluorescence method.

Sample preparation and analysis

Samples were cylindrical (Ø = 50 mm, $L = 100$ mm), each being made with 20% lime and 80% ground sand, with 10% of water added. Blast furnace slag with different specific surface partially replaced the lime. The compaction pressure of samples was 20 MPa. Hydrothermal synthesis was carried out under saturated steam pressure at temperatures of 176, 190 and 204°C, and steam pressures of 1·0, 1·5 and 1·8 MPa. The duration of the treatment in autoclaving was 10 h: that is, 2 h for progressively rising temperatures, 6 h of conservation at constant temperature and finally 2 h for cooling by ventilation. After synthesis, samples were removed from the autoclave. Throughout the curing period, the compressive strength was measured after 2 d.

The XRD data were collected by Philips PW 3710 X-ray diffractometer with Bragg–Brentano geometry using Ni-filtered Cu Kα radiation, operating with the voltage of 30 kV and emission current of 20 mA. The step-scan covers the angular range 2–60° (2θ) in steps of $2\theta = 0{\cdot}02°$. The morphology of hydrates formed was determined by SEM (SEM-JEOL-JSM-6301F) using an accelerating voltage of 9 kV and a working distance of 15 mm. The elementary compositions (EDX) were measured using energy-dispersive spectrometer Oxford Inca Link (SEM JSM 6400).

Results and discussion

Compressive strength

Table 2 shows the compressive strength under the influence of the following effects: replacement rate of hydrated lime by granulated slag, the fineness of the slag and the saturated vapour pressures in autoclave. Replacing hydrated lime by granulated slag as a binder, induces a significant reduction in compressive strength. It is slightly affected when the slag percentage is less than 40% and significantly affected with higher percentages.

Per cent by mass	Silicon dioxide (SiO_2)	Calcium oxide (CaO)	Magnesium oxide (MgO)	Aluminium oxide (Al_2O_3)	Iron (III) oxide (Fe_2O_3)	Titanium dioxide (TiO_2)	Manganese oxide (MnO)	Potassium oxide (K_2O)	Sodium oxide (Na_2O)	Barium oxide (BaO)	Loss on ignition
Slag	35·68	42·17	7·49	7·92	0·5	0·29	3·04	0·51	0·29	1·74	25·35
Lime	0·54	70·53	1·16	—	0·28	—	—	—	—	—	
Sand	96·1	0·18	0·9	1·7	0·83	—	—	0·29	—	—	

Table 1. Chemical analyses of initial compounds

Offprint provided courtesy of www.icevirtuallibrary.com
Author copy for personal use, not for distribution

Saturated vapour pressures in autoclave: MPa	Fineness (slag): cm^2/g	Replacement ratio of slag: %					
		0	20	40	60	80	100
1·0	2500	36·4	30·6	27·3	20·8	14·4	3·2
	3500	36·4	31·1	27·6	24·2	15·8	5·7
	4500	36·4	33·2	29·2	24·3	16·5	7·6
1·5	2500	42·4	36·1	31·4	25·0	17·3	8·0
	3500	42·4	38·3	32·9	27·0	19·9	11·2
	4500	42·4	39·2	33·8	27·5	20·7	12·7
1·8	2500	45·2	40·5	36·1	28·9	19·7	9·8
	3500	45·2	41·1	36·8	30·8	24·1	12·7
	4500	45·2	41·9	38·8	32·3	25·4	14·8

Table 2. Compressive strength (MPa) of samples containing different percentages of slag

The evolution of compressive strength according to the variation of fineness of the granulated slag is reported in Table 2 as well as in Figure 3. This contributes slightly to the increase of the compressive strength when the specific surfaces vary from 2500 to 3500 cm^2/g. The effect is not significant when varying between 3500 and 4500 cm^2/g. In addition, the excessive grinding promotes the formation of electrostatic charges of particles, which produces flocculation. As with the cement case, the phenomenon of over-grinding leads to flocculation phenomena attributed to electrostatic charges, which agglomerate the extremely fine particles (Diederich *et al.*, 2012). In addition, the hydration product of the mechanically activated slag depends not only on the initial specific surface area of the slag but also on the surface activation, as manifested by the change in the zeta potential of the slag during the milling process (Kumar *et al.*, 2005). This explains the low increase of mechanical strength in the specimens composed from slag with specific surface areas between 3500 to 4500 cm^2/g compared to between 2500 and 3500 cm^2/g.

Temperature, related to the autoclaving pressure, contributes to the activation of slag and also ensures an interesting evolution of mechanical resistance (Aldea *et al.*, 2000). On the other hand, the lime in solution increases the pH; consequently the slag is in this highly basic environment. This environment can be depleted (less basic) if the Ca^{++} ions combine with the silica of slag to form the C-S-H.

The mechanical strength is observed to improve significantly when the saturated vapour pressure, inside the autoclave, ranges from 1·0 to 1·5 MPa. On the other hand, for the case of 1·5–1·8 MPa saturated vapour pressure, a slight improvement is noticed (Figure 4). A significant increase of curing temperature can result in the phase breakdown followed by recrystallisation of

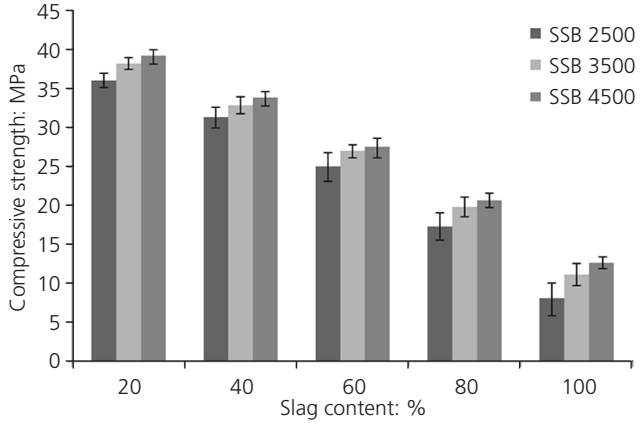

Figure 3. Compressive strength development of samples containing different proportions of slag and autoclaved at saturated vapour pressure to 1·5 MPa

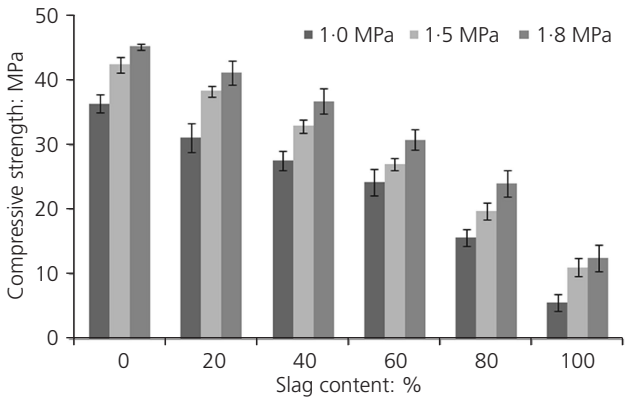

Figure 4. Compressive strength development of samples containing different proportions of slag at specific surface of 3500 cm^2/g

Offprint provided courtesy of www.icevirtuallibrary.com
Author copy for personal use, not for distribution

other phases with weaker properties at microscopic scale (or at crystal scale) (Gutovic *et al.*, 2005). In the work reported by Black *et al.* (2009) concerning xonotlite, which was not general to hydrothermally formed phases, an increasing synthesis temperature led to larger crystals, but the crystals also appeared to have split along their length. This case is also observed in the present study: there is a conversion of the tobermorite to xonotlite. Figure 5 shows well-crystallised tobermorite in the form of dense and entangled platelets, whereas xonotlite is in the form of very fine interwoven needles (Figure 6). However, at material scale the interleaving of xonotlite needles leads to an improvement of mechanical strength.

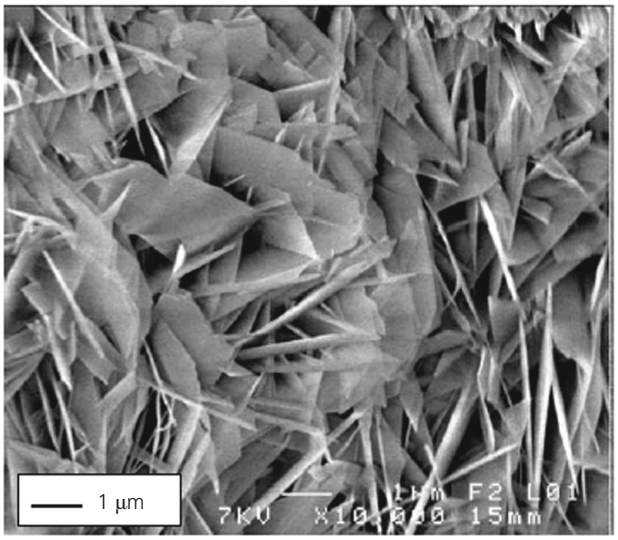

Figure 5. SEM micrograph of 11 nm tobermorite morphology

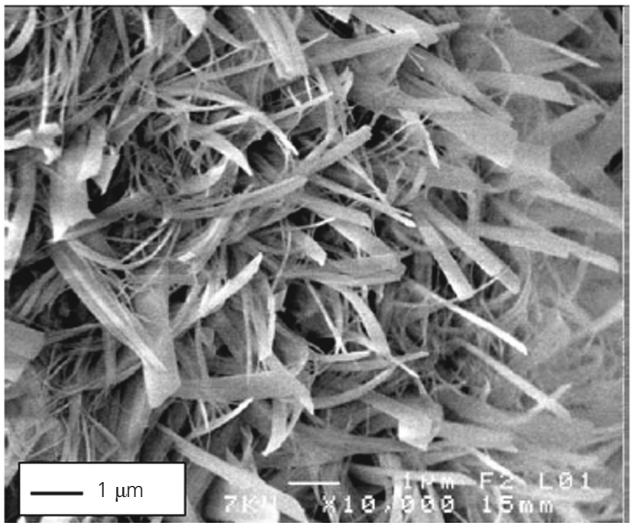

Figure 6. SEM micrograph of xonotlite morphology

Microstructural analyses

Samples containing 0, 40, 60 and 100% of granulated slag (ground to a specific surface of 3500 cm^2/g) were autoclaved at saturated vapour pressures of from 1·0 to 1·8 MPa. Samples were observed using XRD, SEM (SEM) and EDX.

The X-ray powder diffraction patterns (Figures 7 and 8) show a significant presence of portlandite in the sample without slag. The decrease of portlandite is induced by the pozzolanic effect

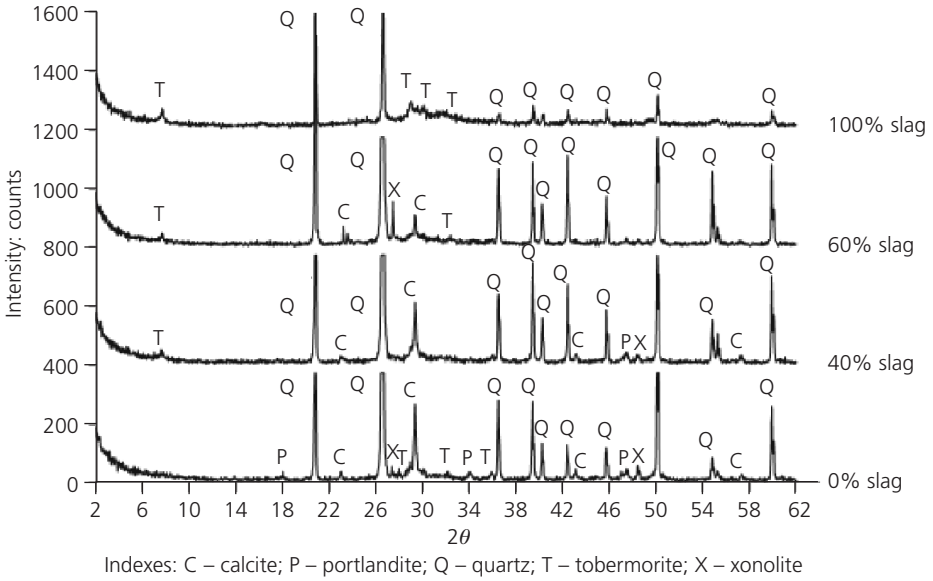

Figure 7. X-ray diffraction patterns of synthesis products at saturated vapour pressure of 1·0 MPa (176°C)

Offprint provided courtesy of www.icevirtuallibrary.com
Author copy for personal use, not for distribution

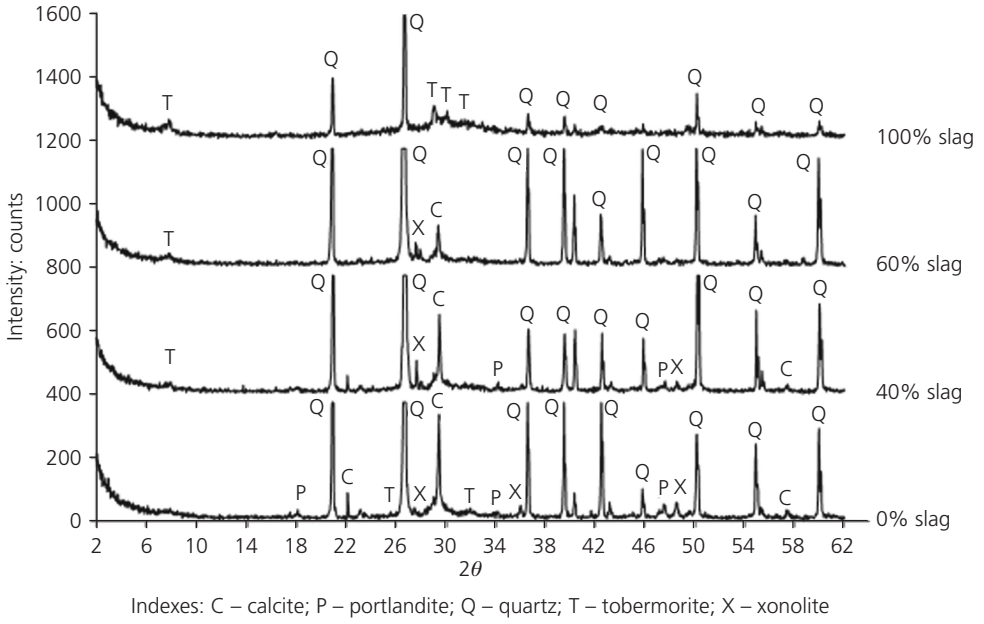

Figure 8. X-ray diffraction patterns of synthesis products at saturated vapour pressure of 1·8 MPa (204°C)

when the slag partially replaces hydrated lime, and is also attributable to dilution. Portlandite disappears completely for mixtures of 60 and 100% granulated slag. In the XRD patterns at the temperatures employed and in the presence of slag, the poorly crystallised phases appear. The spectral line located at 7·8° 2θ is more visible; the XRD patterns from the sample without slag do not show clearly.

The temperature effect, that is autoclaving pressure, is also highlighted; the XRD intensity corresponding to portlandite decreases when the autoclaving pressure reaches 1·8 MPa for a slag-free mixture. This is probably attributable to silica, which reacts with Ca^{++} into solution to produce new hydrated calcium silicates. XRDs at Miller indices (hk0) of C-S-H seem to increase. The presence of tobermorite 11 nm ($C_5S_65H_2O$) and of xonotlite ($C_6S_6H_2O$) is also observed. Their diffraction lines are very weak and perceptible with difficulty. These hydrated calcium silicates are probably in too low quantities to give high intensities compared with XRD of quartz (sand of the mixture). When the curing temperature in the autoclave increases, the formation of xonotlite at the expense of tobermorite is noticed. This is attributed to the presence in the matrix of aluminium. When the latter increases, the tobermorite becomes a more stable phase as the autoclaving temperature decreases. Inversely, when the aluminium contents decrease and the temperature increases, the xonotlite will become the most stable phase. The EDX data analyses (Tables 3 and 4) confirm this; Shaw *et al.* (2000) also reported this observation. The presence of the slag does not

Oxide: % by mass	Samples			
	0% slag	40% slag	60% slag	100% slag
Aluminium oxide (Al_2O_3)	3·16	3·07	11·00	3·10
Silicon dioxide (SiO_2)	54·90	42·37	43·29	50·89
Calcium oxide (CaO)	41·94	50·92	38·79	40·89
Magnesium oxide (MgO)	—	5·27	5·92	4·11
Iron (III) oxide (Fe_2O_3)	—	—	—	—
Potassium oxide (K_2O)	—	—	0·41	—
Calcium oxide (CaO)/silicon dioxide (SiO_2) ratio	0·75	1·2	0·9	0·8

Table 3. EDX of newly formed hydrates in autoclave at temperature of 176°C

Offprint provided courtesy of www.icevirtuallibrary.com
Author copy for personal use, not for distribution

Oxide: % by mass	Samples			
	0% slag	40% slag	60% slag	100% slag
Aluminium oxide (Al_2O_3)	1·67	6·03	5·56	–
Silicon dioxide (SiO_2)	57·30	60·91	71·8	36·25
Calcium oxide (CaO)	41·03	32·59	22·54	54·07
Magnesium oxide (MgO)	—	—	—	9·69
Iron (III) oxide (Fe_2O_3)	—	—	—	—
Potassium oxide (K_2O)	—	0·35	—	—
Calcium oxide (CaO)/silicon dioxide (SiO_2) ratio	0·72	0·54	0·32	1·49

Table 4. EDX of newly formed hydrates in autoclave at temperature of 204°C

provide new phases of distinct hydrates on the XRD patterns, whereas the tobermorite is clearly present, especially regarding mixtures with 100% slag.

To appreciate the new phases formed, it is necessary to use SEM (Figures 9–12). Figure 9(a) shows the tobermorite in the form of dense and entangled well-crystallised platelets. Xonotlite is in the form of very fine interwoven needles (Figure 9(b)). These two aspects are the usual forms of tobermorite and xonotlite. They try to overrun the cracks and cleave slightly in some cases. Some atomic directions of the unit cell of the initial crystal network with a development in platelets are conserved in the crystal network of the xonotlite. This leads to cleavages (cracks of parallel orientation fixed by the initial atomic network). The fibres of the resulting xonotlite occurred in parallel laths in the form of a bundle (observations by HFW Taylor in the 1960s) (Speakman, 1968). The addition of 40% slag in lime substitution did not disturb the fundamental aspect of these two phases (Figures 10(a) and 10(b)). On the other hand, with 60% slag at autoclave temperatures of 176 and 204°C, the phases obtained show cleavages that have fibrous aspects (Figures 11(a) and 11(b)). The fibres develop on the slag particle and progress into the porosity. Finally, with 100% slag the phases obtained have needle-like appearances. The germination appears to occur on particles of slag showing a fibred structure with a characteristic sea-urchin shape (Figure 12(a)). At a temperature of 204°C, the

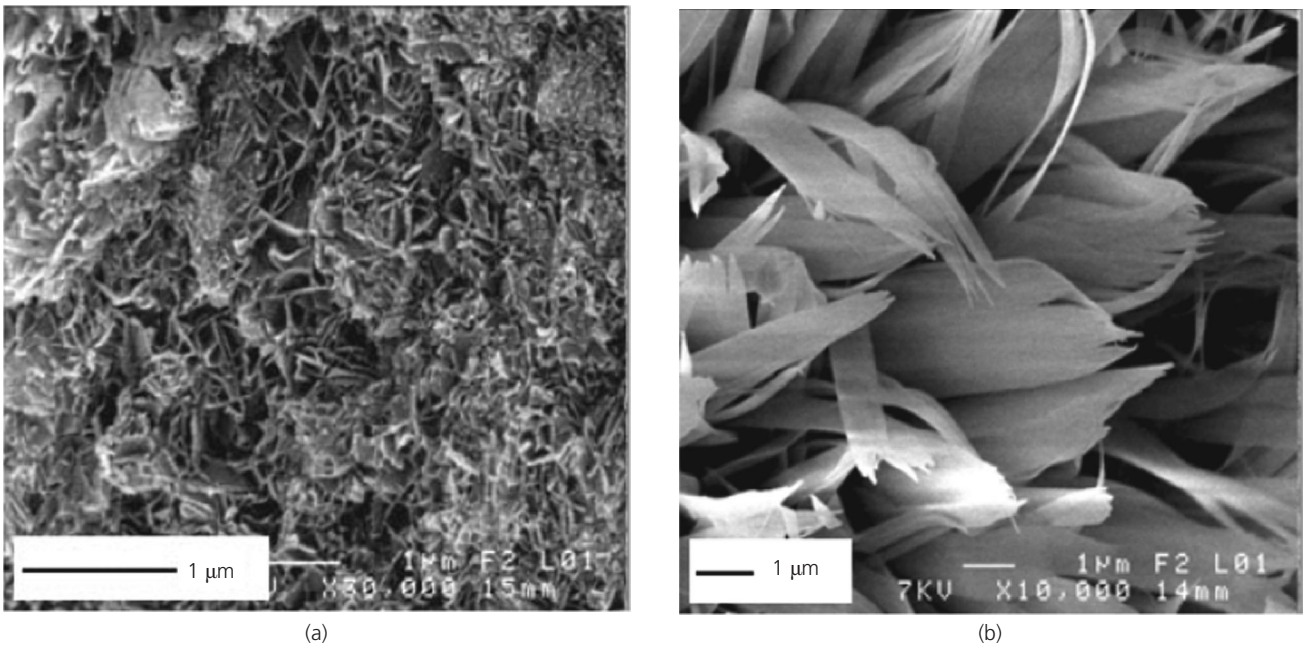

(a) (b)

Figure 9. SEM micrographs of samples containing 0% slag: (a) sample treated at 176°C; (b) sample treated at 204°C

Offprint provided courtesy of www.icevirtuallibrary.com
Author copy for personal use, not for distribution

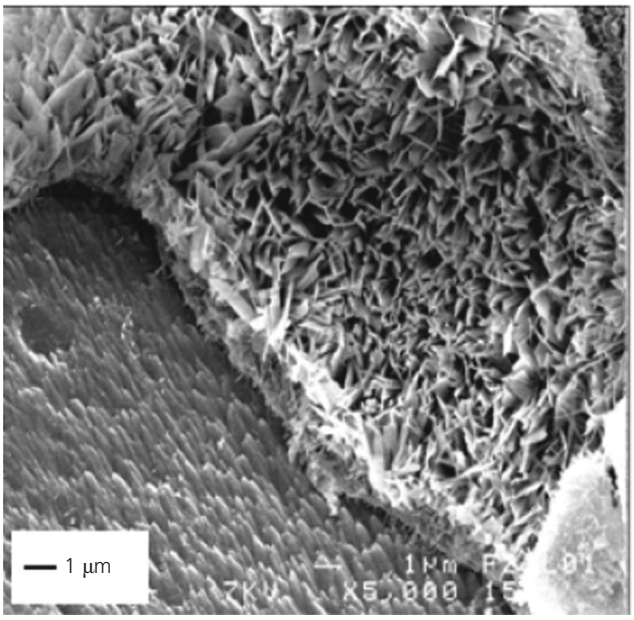

(a)

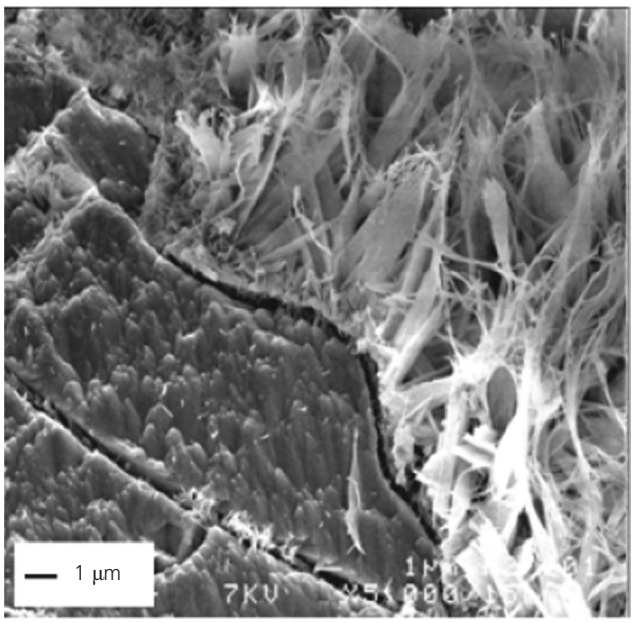

(b)

Figure 10. SEM micrographs of samples containing 40% slag: (a) sample treated at 176°C; (b) sample treated at 204°C

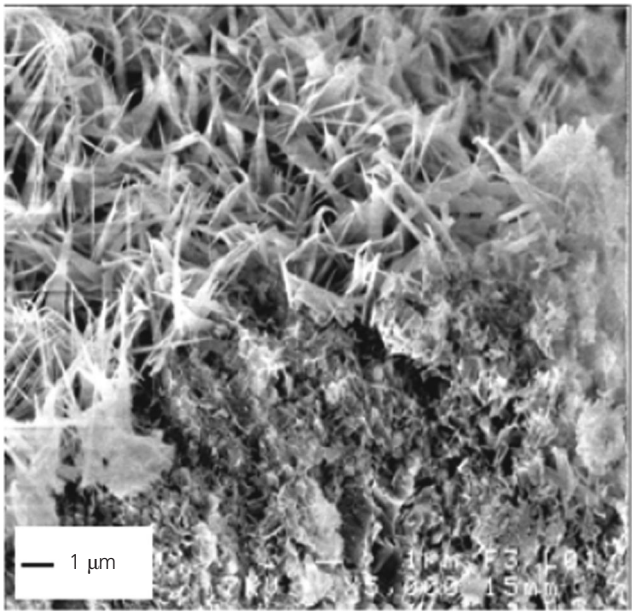

(a)

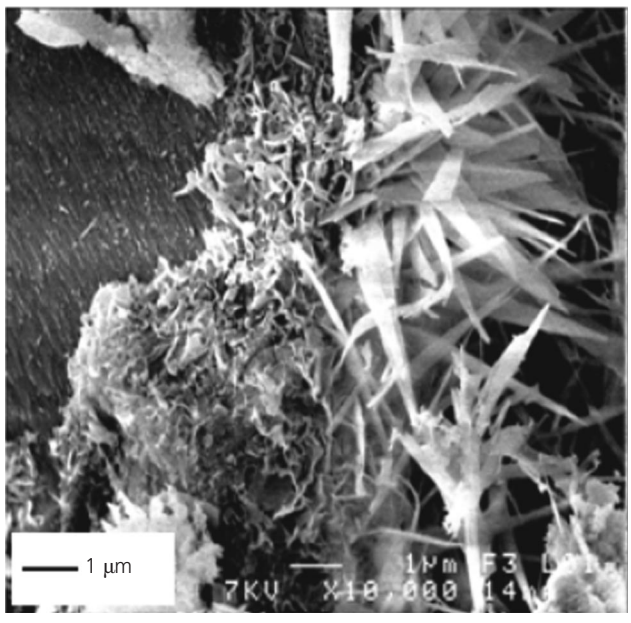

(b)

Figure 11. SEM micrographs of samples containing 60% slag: (a) sample treated at 176°C; (b) sample treated at 204°C

form of the phases is as fine needles (Figure 12(b)). The cleavage of phases which occurs presents a different appearance to products obtained with the samples containing 40 and 60% slag. The EDX data analyses that identify the hydrates formed are given in Tables 3 and 4. The investigation cannot resolve the ambiguity: tobermorite or xonotlite. These two hydrates are composed of the same elements (oxides). The C/S ratio mean is approximately equal to 0·85. Overall, the atomic elements noticed in EDX analyses correspond to the presence of C-S-H. Other elements such as magnesium, potassium and iron are also present, but in small quantities introduced to the mix by granulated slag.

Conclusions

The complexity of the calcium oxide–silicon dioxide–water system under hydrothermal reaction and saturated vapour pressure has been widely discussed for many years. The presence of

Offprint provided courtesy of www.icevirtuallibrary.com
Author copy for personal use, not for distribution

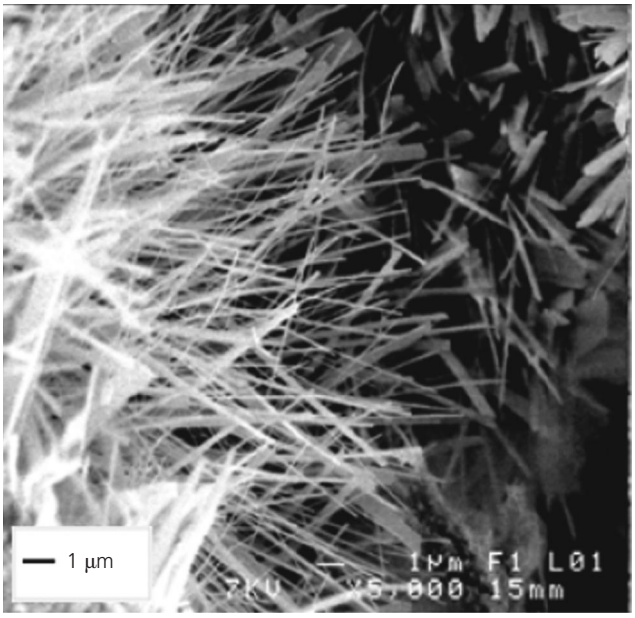

(a)

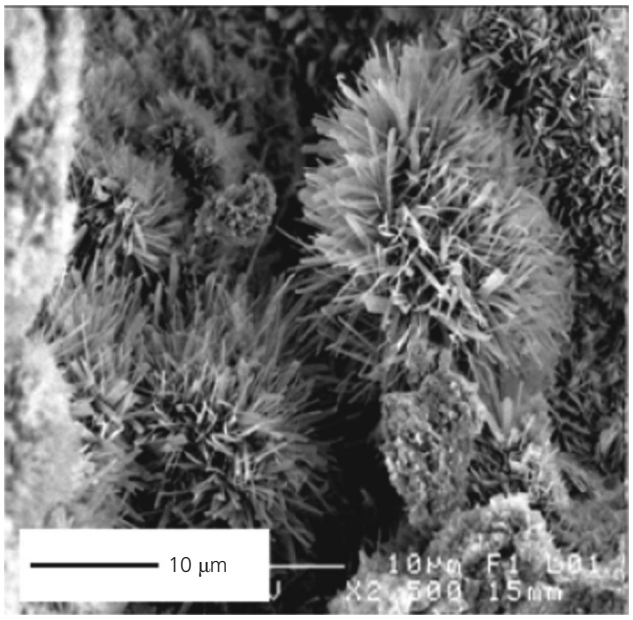

(b)

Figure 12. SEM micrographs of samples containing 100% slag: (a) sample treated at 176°C; (b) sample treated at 204°C

slag with almost a complete amorphous structure under such conditions, does not release new hydrate phases other than those known in similar conditions.

It is estimated that a relatively high concentration of calcium ions is required for hydrate formation; the presence of lime is found to be essential as an activator for slag.

The mechanical strengths are closely related to composition of mixtures. It is estimated that the increment of temperature does not significantly affect resistance (in this study). However, the temperature has a much greater influence on the morphology and crystalline structure of C-S-H.

The increase in the fineness of the grinding of slag has not brought the desired effect on the mechanical resistance with small amounts of slag (20% of total mixture).

The investigation of phases by X-ray diffractograms is complicated by the presence of quartz (well crystallised and with intensities that mask other phases). However, the SEM micrographs are more clearly highlighted.

The usual forms of tobermorite and xonotlite are distinct and are not disturbed by the presence of slag. Atomic elements such as aluminium, iron, potassium, magnesium and sodium are present but they do not affect the areas of synthesis and stability of these phases.

Acknowledgements

The authors express their thanks to Joseph Le Lannic and Francis Goutefangeas, CMEBA Rennes1 University (France), for their assistance with SEM.

REFERENCES

Aitken A and Taylor HFW (1960) Hydrotermal reactions in lime-quartz pastes. *Journal of Applied Chemistry* **10(1)**: 7–15.

Aldea CM, Youngb F, Wanga K and Shaha SP (2000) Effects of curing conditions on properties of concrete using slag replacement. *Cement and Concrete Research* **30(3)**: 465–472.

Al-Wakeel EI, El-Korashy SA, El-Hemaly SA and Uossef N (1999) Promotion effect of C-S-H phase nuclei on building calcium silicate hydrate phases. *Cement and Concrete Composites* **21(3)**: 173–180.

Baltakys K, Jauberthie R and Kasperaviciute V (2009) Formation and stability of C–S–H(I) in CA (OH) 2/CaO–thermal silica densified–H_2O system. *Journal of Ceramics-Silikáty* **53(2)**: 81–87.

Barnett SJ, Soutsos MN, Millard SG and Bungey JH (2006) Strength development of mortars containing ground granulated blast-furnace slag: effect of curing temperature and determination of apparent activation energies. *Cement and Concrete Research* **36(3)**: 434–440.

Behim M, Cyr M and Clastres P (2011) Physical and chemical effects of El Hadjar slag used as an additive in cement-based materials. *European Journal of Environmental Civil Engineering* **15(10)**: 1413–1432.

Black L, Garbev K and Stumm A (2009) Structure bonding and morphology of hydrothermally-synthesised xonotlite. *Advances in Applied Ceramics* **108(3)**: 137–144.

Chen JJ, Thomas JJ, Taylor HFW and Jennings HM (2004) Solubility and structure of calcium silicate hydrate. *Cement and Concrete Research* **34(9)**: 1499–1519.

Crennan JM, El-Hemaly SA and Taylor HFW (1977) Autoclaved

Offprint provided courtesy of www.icevirtuallibrary.com
Author copy for personal use, not for distribution

lime–quartz materials I. Some factors influencing strength. *Cement and Concrete Research* **7(5)**: 493–502.

Diederich P, Mouret M, De Ryck A, Ponchon F and Escadeillas G (2012) The nature of limestone filler and self-consolidating feasibility—relationships between physical, chemical and mineralogical properties of fillers and the flow at different states, from powder to cement-based suspension. *Powder Technology* **218(March)**: 90–101.

Dietz T and Bohnemann K (2000) Calcium silicate hydrate in fiber cement sheets and autoclaved aerated concrete (AAC). *Proceedings of 7th International Conference on Inorganic-Bonded Wood and Fiber Composite Materials, Sun Valley, Idaho, USA*, pp. 1–13.

Gruskovnjak A, Lothenbach B, Winnefeld F *et al.* (2008) Hydration mechanisms of super sulphated slag cement. *Cement and Concrete Research* **38(7)**: 983–992.

Gutovic M, Klimesch DS and Ray A (2005) Strength development in hydrothermally treated OPC: CB systems. *Journal of Thermal Analysis and Calorimetry* **80(3)**: 631–635.

Hong SY and Glasser FP (2004) Phase relations in the $CaO–SiO_2–H_2O$ system to 200°C at saturated steam pressure. *Cement and Concrete Research* **34(9)**: 1529–1534.

Jauberthie R, Temimi M and Laquerbe M (1996) Hydrothermal transformation of tobermorite gel to 10 Å tobermorite. *Cement and Concrete Research* **26(9)**: 1335–1339.

Klimesch DS and Ray A (2002) Evaluation of phases in a hydrothermally treated $CaO–SiO_2–H_2O$ system. *Journal of Thermal Analysis and Calorimetry* **70(3)**: 995–1003.

Kondo R (1965) Kinetic study on hydrothermal reaction between lime and silica. *Proceedings of 1st International Symposium on Autoclaved Calcium Silicate Building Products, London, UK*, pp. 92–97.

Kumar R, Kumar S, Badjena S and Mehrotra SP (2005) Hydration of mechanically activated granulated blast furnace slag. *Metallurgical and Materials Transactions B* **36(6)**: 873–883.

Narayanan N and Ramamurthy K (2000) Structure and properties of aerated concrete: a review. *Cement and Concrete Composites* **22(5)**: 321–329.

Richardson IG (2008) The calcium silicate hydrates. *Cement and Concrete Research* **38(2)**: 137–158.

Shaw S, Clark SM and Henderson CMB (2000) Hydrothermal formation of the calcium silicate hydrates, tobermorite ($Ca_5Si_6O_{16}(OH)_2 \cdot 4H_2O$) and xonotlite ($Ca_6Si_6O_{17}(OH)_2$): an in situ synchrotron study. *Chemical Geology* **167(1–2)**: 129–140.

Siauciunas R and Baltakys K (2004) Formation of gyrolite during hydrothermal synthesis in the mixtures of CaO and amorphous SiO_2 or quartz. *Cement and Concrete Research* **34(11)**: 2029–2036.

Speakman K (1968) *The Stability of Tobermorite in the System $CaO-SiO_2-H_2O$ at Elevated Temperatures and Pressures*. Building Research Station, Gaston, Watford, Herts, UK, pp. 1090–1103.

Taylor HFW (1997) *The Chemistry of Cement*, 2nd edn. Thomas Telford Publishing, London, UK.

Ungkoon Y, Sittipunt C, Namprakai P *et al.* (2007) Analysis of microstructure and properties of autoclaved aerated concrete wall construction materials. *Journal of Industrial Engineering Chemistry* **13(7)**: 1103–1108.

Yazıcı H, Deniz E and Baradan B (2013) The effect of autoclave pressure, temperature and duration time on mechanical properties of reactive powder concrete. *Construction and Building Materials* **42(May)**: 53–63.

WHAT DO YOU THINK?

To discuss this paper, please submit up to 500 words to the editor at journals@ice.org.uk. Your contribution will be forwarded to the author(s) for a reply and, if considered appropriate by the editorial panel, will be published as a discussion in a future issue of the journal.